Zygomatic Root Position in Recent and Fossil Hominids

GERHARD W. WEBER[1,2]* AND VIKTORIA A. KRENN[1,2]
[1]Department of Anthropology, University of Vienna, Austria
[2]University of Vienna, Core Facility for Micro-Computed Tomography, Austria

ABSTRACT

The relative position of the zygomatic root to the dentition plays a crucial role in determining the overall strength of the face in response to bite forces. The powerful superficial head of the masseter arises there and the zygomaticoalveolar crest (ZAC) is discussed as a buttressing feature of the face. For instance, a more forwardly or backwardly positioned zygomatic root or a lower or higher vertical distance to the dentition could be indicative for evolutionary adaptations to particular loading regimes which are associated with diet. We therefore examined the morphology of the maxilla using state-of-the-art 3D Geometric Morphometric methods. The data set was reduced to a minimum of relevant measurements and includes five landmarks (pr, ol, zm, lingual and buccal midpoint of second molar alveoli) and three curves with semilandmarks along the lingual and buccal alveolar rim and the ZAC. Results show a stunning overlap in shape variation. We find no clear pattern of shape that would allow separating different hominid groups with confidence, except two extreme forms—Paranthropines and Neanderthals. We also find no clear trend over time. Australopithecines, Habilines, Erectines, and Middle Pleistocene *Homo* can be very similar to modern humans. Even great apes are within or not far from the central shape distribution of *Homo*, but they separate clearly from gracile and robust Australopithecines. We discuss the shape factors underlying our data. The geometry studied allows simple measurements and analyses and is thus potentially interesting for classification purposes of extreme forms. Anat Rec, 300:160–170, 2017. © 2016 Wiley Periodicals, Inc.

Key words: zygomatic process; maxilla; zygomatic arch; zygomaticoalveolar crest; human evolution; buttress; biomechanics; mastication

INTRODUCTION

Cranial diversity among primates is largest in hominoids, particularly if *Homo sapiens* is included (Fleagle et al. 2010). The modern human cranium is characterized by a large globular braincase and a retracted face with a small jaw (Lieberman 2011), while extant apes such as *Pan troglodytes, Gorilla gorilla* or *Pongo pygmaeus*, as well as most Australopithecines (except *Au. sediba*), show a marked facial prognathism. With early members of the genus *Homo* the face became more orthognathic, narrower and taller, but Mid-Pleistocene *Homo* still exhibits considerable prognathism. The maxillary bone shows mainly depository bone remodeling in

Associate Editor: Prof. Jeffrey T. Laitman

Grant sponsors: Oesterreichische Nationalbank, Anniversary Fund; Grant number: 16121.

*Corresponding author: Univ. Prof. Dr. Gerhard W. Weber, Department of Anthropology & Core Facility for Micro-Computed Tomography, University of Vienna, Althanstr. 14, A-1090 Wien, Austria, Tel: +43-1-4277-54701, Fax: +43-1-4277-9547, Email: gerhard.weber@univie.ac.at

Received 14 March 2016; Revised 1 June 2016; Accepted 14 June 2016.

DOI 10.1002/ar.23490
Published online in Wiley Online Library (wileyonlinelibrary.com).

Pliocene and early Pleistocene hominins, while modern humans exhibit extensive bone resorption (Lacruz et al. 2015). All together, we can recognize a reduction in size and robusticity of the face, the postcanine dentition, and the chewing forces in the genus *Homo* (Demes & Creel 1988; McHenry & Coffing 2000; Lieberman 2011). Likely reasons for the masticatory reduction are dietary shifts along the way from Australopithecines to early *Homo*, Middle Pleistocene *Homo*, and modern humans (Rak 1983; Brace et al. 1987; Wrangham et al. 1999; Lieberman 2008; Ungar et al. 2006; Lucas 2004; Wrangham & Carmody 2010; Ungar 2012). Easier digestible food and the invention of extra-oral food processing techniques (e.g. tool use, cooking) are reasonable factors discussed in hominin evolution leading to a reduction of loading regimes related to mastication (Lucas 2004; Lieberman et al. 2004; Zink et al. 2014).

The zygomatic (malar) process of the hominid maxilla is the anterior root of the zygoma and connects via a rough articulation surface with the zygomatic bone. The latter joins posteriorly with the zygomatic process of the temporal bone. One of the most powerful muscles of the skull, the superficial head of the masseter, arises by a thick, tendinous aponeurosis from the zygomatic process of the maxilla and from the anterior two-thirds of the inferior border of the zygomatic arch. Its fibers pass inferior and posterior to insert into the angle of the mandible and the inferior half of the lateral surface of the ramus of the mandible. Other muscles originating in the region of the zygomatic root are mimic muscles, such as the musculus levator anguli oris, the musculus zygomaticus, and the musculus caninus (Fig. 1).

The location of the zygomatic root, particularly its relative position to the postcanine dentition where major strains during chewing occur, certainly plays a crucial role in determining the overall strength of the face in response to bite forces (Ledogar et al. 2016b, this volume). The whole zygomatic arch is a functional requirement and surely not an anachronistic relic of phylogeny (Witzel et al. 2004). It has to sustain bite forces, it must withstand bending in a plane parallel to the occlusal plane, and it also redirects tensile forces produced by the masseter and the temporal fascia. Facial dimensions, e.g. a more forward or backward position of the zygomatic root as well as a wider or narrower mid-face, influence the pattern of stresses and strains which the face experiences during chewing (Hylander 1977). Furthermore, the position of the zygomatic root influences the mechanical advantage of the superficial head of the masseter which elevates the mandible. Due to its diagonal direction, it also moves the mandible forward (protrusion).

It seems reasonable to assume that the position of the zygomatic root in relation to the dentition might reflect evolutionary adaptations in response to biomechanical demands. For instance, Rak (1983) advocated that the placement of the zygomatic root relative to the rostrum might influence the strain patterns in the Australopithecine face, particularly a laterally expanded zygomatic root together with a straight and steeply-inclined zygomaticoalveolar crest (see below) would act as a bony buttress (cf. anterior pillars in some Australopithecines and Paranthropines). Tracing the inferior border of the zygoma from posterior to anterior, in many hominids a more or less sharp ridge is easily detected. At the most inferior point of the *sutura zygomaticomaxillaris* [zygomaxillare (zm)] there is often a well-palpable crest running down the lateral wall towards the alveolar process of the maxilla. In other cases only a slightly elevated, rounded column that fades out long before reaching the alveoli can be seen. The crest is called the "zygomaticoalveolar crest" (ZAC; Rak 1983; synonymous with "crista zygomaticoalveolaris") or "inferior zygomaticomaxillary margin" (IZM; Pope 1991). Both authors focused on the curvature of this crest and on its height in relation to the dental arch in Australopithecines, early *Homo*, and modern humans. The zygomaxillary region in Neanderthals is tall and swept back (Rak 1986) which contributes to their typical appearance of the midface. Trinkaus (1987) described a posterior migration of the zygomatic root in Neanderthals compared to Middle Pleistocene hominids and Proto-Neanderthals as one factor determining this distinct configuration. The zygomatic root in Neanderthals arises typically above second to third molar (M^2-M^3; Trinkaus 1987) rather than first to second molar (M^1-M^2; Lieberman 2011).

Today, by 3D measurements, structures can be related to each other considering their actual spatial geometry quantitatively. From a functional-morphological view on hominid evolution, two questions with regard to the relative position of the anterior root of the zygoma can be raised: 1) where in anterior-posterior direction is its location relative to the postcanine dentition, and 2) how is the zygomaticoalveolar crest shaped, which includes the height of the zygomatic root above the alveolar plane? The location of the zygomatic root is often found between M^1 or M^2 (e.g., in recent humans, see also Lieberman 2011), but can be also seen above the premolars (e.g., in Paranthropines), or between M^2 and M^3 (e.g., in Neanderthals). Using advanced morphometric methods, some authors dealt implicitly with the topic, e.g. by studying the face of Middle Pleistocene hominins, and found temporal clusters between them (Freidline et al. 2012). Unfortunately, in this study the question of the relative position of the anterior zygoma was not explicitly addressed. Noback and Harvati (2015) recently published works on cranial shape to investigate its relation to subsistence. Their 3D measurements included a subset capturing the dental arch and zygomatic root, but their sample focused on modern humans only. Beside a few studies touching the topic, there is a lack in literature using state-of-the-art technologies to answer the questions raised above. This prompted us to address the issue if a clear evolutionary trend (probably even useful for classification purposes) exists, or if we find rather an inconsistent pattern of variation across hominid taxa.

Our study is a first attempt to examine the morphology of the maxilla with regard to the relative position of the zygomatic process to the dentition by Geometric Morphometric methods. The data set was reduced to a minimum of relevant measurements to include as many as possible recent and fossil specimens. Our goal is to provide results on the existing variation in extant modern humans and apes, and in some extinct hominin taxa.

MATERIALS AND METHODS

The sample to cover morphological trends across different hominid taxa included extant apes [*Pan troglodytes* (Pt; n = 3), *Gorilla gorilla* (Gg; n = 3), *Pongo*

TABLE 1. Specimens in the sample.

Specimen	Group	Origin	Dataorigin	Resolution	Side	TMJ	ZAC
A.L.444-2	**Au**	Ethiopia	medCT (reco S. Senck)	410µm	l	+	M1
MH 1	**Au**	South Africa	medCT	469µm	l	+	<M1
Sts 5	**Au**	South Africa	medCT	390µm	l	+	M1-M2
Sts 71	**Au**	South Africa	medCT	390µm	r	+	M1
KNM-ER 406	**Pa**	Kenya	medCT	390µm	l	+	P4
KNM-WT 17000	**Pa**	Kenya	medCT	330µm	l	+	P4-M1
OH 5	**Pa**	Tanzania	medCT (reco Benazzi et al. (2011))	480µm	l	+	P4
SK 12	**Pa**	South Africa	medCT	290µm	r	–	P3-P4
KNM-ER 1813	**Ha**	Kenya	medCT	254µm	r	+	<M1
Stw 53	**Ha**	South Africa	cast (Anthro Vienna)	Microscribe	r	–	M1
KNM-WT 15000	**Er**	Kenya	medCT	330µm	l	+	P4-M1
Sinanthropus pek.	**Er**	China	cast (reco Sawyer & Tattersall)	Microscribe	l	–	M2
Arago 21	**MPH**	France	cast (Anthro Vienna)	Microscribe	r	–	M1
Atapuerca H5	**MPH**	Spain	medCT	480µm	l	+	M1
Kabwe 1	**MPH**	Zambia	cast (Wenner Grenn 25.522)	Microscribe	l	–	M2
Petralona 1	**MPH**	Greece	medCT	500µm	r	+	M1
Amud 1	**NEA**	Israel	µCT	200µm	l	+	M1-M2
Saccopastore 1	**NEA**	Italy	cast (Anthro Vienna)	Microscribe	l	–	<M2
Saccopastore 2	**NEA**	Italy	cast (Anthro Vienna)	Microscribe	l	–	M2>
Saint Cesaire	**NEA**	France	cast (B. Vandermersch)	Microscribe	r	–	M2-M3
Shanidar 1	**NEA**	Iraq	cast (Smithsonian Institution)	Microscribe	l	–	M2
Jebel Irhoud 1	**eAMH**	Morocco	cast (Meyer Sammlung)	Microscribe	l	–	<M2
Qafzeh 9	**eAMH**	Israel	µCT	200µm	r	+	M2
Skhul 4	**eAMH**	Israel	µCT	90µm	l	–	M1
Skhul 5	**eAMH**	Israel	medCT	480µm	l	+	M1
Ain Mallaha H23	**upMH**	Israel	µCT	75µm	l	–	M1
Brno 3	**upMH**	Czech Rep.	cast (Pöch G239)	Microscribe	r	–	M1
Combe Capelle	**upMH**	France	cast (Dr. F. Krantz G376)	Microscribe	l	–	M1
Dolni Vestonice 3	**upMH**	Czech Rep.	cast (Unterwisternitz)	Microscribe	l	–	M1
Liujiang	**upMH**	China	surface scan	344 kfaces	r	+	P4-M1
Mladec 1	**upMH**	Czech Rep.	medCT	400µm	r	+	M1
Ohalo II H1	**upMH**	Israel	µCT	200µm	l	+	M1
Predmosti 3	**upMH**	Czech Rep.	cast (Pöch G234)	Microscribe	l	–	M1
BLZ_483	**RMH**	Bedouin	µCT	75µm	r	–	M1-M2
C102	**RMH**	Australia	µCT	100µm	l	+	M1-M2
C54	**RMH**	Australia	µCT	100µm	l	+	M1-M2
CN230	**RMH**	Papuan	µCT	100µm	l	+	<M2
CN264	**RMH**	Papuan	µCT	100µm	l	+	M1>
ID_122_199_961	**RMH**	Austria	µCT	100µm	l	+	M1
ID_122_335_1376	**RMH**	Java	µCT	100µm	l	+	M1
ID_122_342_1383	**RMH**	Java	µCT	100µm	l	+	M1
ID_122_421_1464	**RMH**	Africa	µCT	100µm	l	+	M1
ID_122_511_1555	**RMH**	Italy	µCT	100µm	r	+	M1
ID_127_622_1200	**RMH**	Europe	µCT	100µm	r	+	M1
MN735	**RMH**	Africa	µCT	100µm	r	+	M1
NN_1	**RMH**	Bedouin	µCT	50µm	r	–	M1
S103	**RMH**	Khoesan	µCT	75µm	l	–	M1
S121	**RMH**	Khoesan	µCT	75µm	l	–	M1
S85	**RMH**	Africa	µCT	100µm	l	+	M1
VA_26	**RMH**	Asia	µCT	100µm	l	+	M1>
Gorilla_3112	**Gg**	Zaire	µCT	200µm	r	+	M1>
Gorilla_3114	**Gg**	Congo	µCT	200µm	l	–	M1
Gorilla_3119	**Gg**	Congo	µCT	250µm	l	+	M2
Pan_13528	**Pt**	Sierra Leone	µCT	250µm	l	+	M1-M2
Pan_25124	**Pt**	Zoo Wien	µCT	250µm	l	+	M2
Pan_793	**Pt**	Zoo London	µCT	250µm	l	+	M1
Pongo_28801	**Pp**	Zoo Wien	µCT	250µm	l	+	M1-M2
Pongo_3108	**Pp**	Sumatra	µCT	250µm	l	+	M2
Pongo_657	**Pp**	Indonesien	µCT	250µm	r	+	M1-M2
Pongo_658	**Pp**	Indonesien	µCT	250µm	l	+	M1

Group abbreviations:
Pan troglodytes - Pt; Gorilla gorilla - Gg; Pongo pygmaeus – Pp; recent humans - RMH; upper Paleolithic modern humans - upMH; early anatomically modern humans - eAMH; Neanderthals - NEA; Middle Pleistocene hominins - MPH; Erectines - Er; Habilines - Ha; Paranthropines - Pa; Australopithecines – Au.
Other abbreviations:
medCT – medical Computed Tomography; µCT – micro-Computed Tomography; TMJ – temporomandibular joint measured yes (+) or no (-); ZAC - position of the crista zygomaticoalveolaris (or its prolongation towards the alveolar process) relative to tooth position; e.g. “M1” means the crista runs to the middle of the first molar, “M1-M2” means the crista runs to the interspace between first and second molar, “<M1” means the crista runs to the mesial side of the first molar, “M1>“means the crista runs to the distal side of the first molar.
l – left; r – right; P3 – upper third premolar; P4 – upper fourth premolar; M1 – upper first molar; M2 – upper second molar; M3 upper third molar.

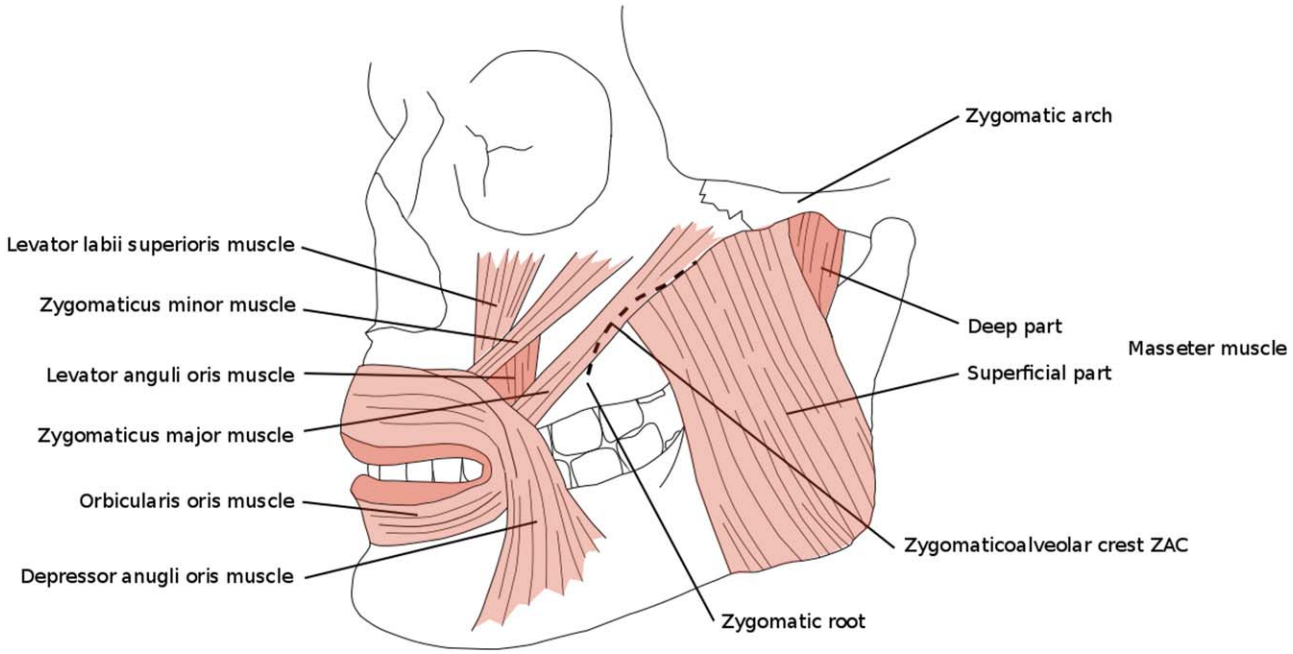

Fig. 1. The zygomatic process of the maxilla and related muscles.

pygmaeus (Pp; n = 4)], recent humans from different geographical populations [*RMH*; Africa, Asia, Australia, Europe, (n = 17)], upper Paleolithic modern humans (upMH; n = 8), early anatomically modern humans (*eAMH*; n = 4), Neanderthals (NEA; n = 5), Middle Pleistocene hominins (MPH; n = 4), Erectines (Er; n = 2), Habilines (Ha; n = 2), Paranthropines (Pa; n = 4), and Australopithecines (Au; n = 4). The labels given here are broad on purpose, since we do not intend to focus on deeper taxonomic affiliation, as for instance would be possible for *Homo heidelbergensis* vs. Protoneanderthals, *H. erectus* vs. *H. ergaster*, etc. (see Tab. 1).

Measurements were taken from either virtual specimens (Computed Tomography - CT, Micro-Computed Tomography - μCT, Surface Scan - SS), or from casts (CA).

Materials came from collections of the University of Vienna, the Natural History Museum Vienna, the Medical University of Vienna, the Tel Aviv University, the Aristotle University of Thessaloniki, the Universidad Complutense de Madrid, the University of the Witwatersrand, the National Museums of Kenya, the Transvaal Museum, the National Museum of Tanzania, the National Museum of Ethiopia, the Natural History Museum London, and the Institute of Vertebrate Paleontology and Paleoanthropology China.

Osteological materials were either scanned using medical CTs at different facilities (in some cases by colleagues who made scans available), or surface scanned (see Tab. 1 for resolution). Most μCT data were scanned at the Core Facility for Micro-Computed Tomography at University of Vienna with a custom built VISCOM X8060 (Germany) μCT-scanner with slightly differing scan parameters (adjusted for each specimen): 110-140kV, 280-520μA, 1400-2000msec, diamond high performance transmission target, 0.5-1.00mm copper filter. X-ray images were taken from 1440 different angles with a pixel size between 50-80μm. Using filtered back-projection in VISCOM XVR-CT 1.07 software, these data were reconstructed as 3D volumes with a color depth of 16,384 grey values and resolutions between 50-250μm.

Post-processing of the image stacks was performed in AMIRA 5.6 (Mercury Computer Systems, Chelmsford, USA), generating 3D surface models of the maxilla. Landmarks and curves were collected in Amira and RapidForm XOR2 64 SP1 (www.rapidform.com). The data operations followed the guidelines from the textbook "Virtual Anthropology" (Weber & Bookstein 2011, see also Weber 2015). Casts were measured with a Microscribe 2GX, producing only landmark and curve data, but no surfaces or volumes. The casts were fixed upside down in Frankfurt Horizontal plane, to make all landmarks accessible. Measurements were taken three times and we proceeded with the data set closest to the mean. All curves were converted into splines in RapidForm XOR2 64 SP1 and smoothed.

Measurements of fossil specimens are often problematic due to the fragmentary preservation or the impossibility to identify landmarks on either the virtual specimen or the cast. In this study the Neanderthal sample was particularly difficult to obtain since most specimens lack maxillary anatomy either on the anterior portion, on the zygomatic process, or on both. For this study the location of landmarks on one half of the face was sufficient and analyses were restricted to the left side. Only in cases of a poor state of preservation of the left side, we mirrored the right side. This enhances the small sample size which in our opinion outweighs the potential disadvantage of omitting facial asymmetries.

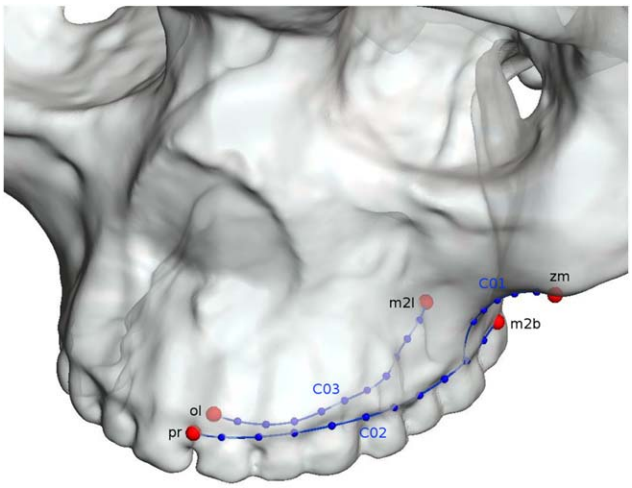

Fig. 2. Measured landmarks and semilandmarks on curves (for abbreviations see text).

The set of landmarks and semilandmarks on curves compromises between sample size and relevant morphological information. Fig. 2 shows the set of measurements. Traditional landmarks (LM) were taken from the anterior portion of the maxilla on the Prosthion (pr) and the Orale (ol). Both landmarks also act as starting points for the curves along the alveolar rim buccally (C02) and lingually (C03), respectively. To obtain further landmarks on the posterior maxilla, we measured the mid-point of the M^2 alveolar socket (measurable even in case of a lost tooth as the alveoli is still present) buccally (m2b) and lingually (m2l). These points determined the end of the curves along the alveolar rims. Focusing on the M^2 avoided common problems with impacted, rotated, missing or malformed M^3s, and on the other hand stretched the curves over a maximum distance along the dental arch beyond M^1. The fifth landmark Zygomaxillare (zm) provided the location of the connection between the malar process of the maxilla and the os zygomaticum at the inferior border of the *sutura zygomaticomaxillaris*. From zm we traced a curve (C01) following the crista zygomaticoalveolaris, or its equivalent faint elevation to its fading approximately in the middle of the anterior surface. The curve was extended to the alveolar rim (but sliding semilandmarks were only placed between zm and the transition between the visible crest and the anterior surface of the maxilla, see Fig. 2). In eighteen cases a landmark or curve had to be placed on minor reconstructions, e.g., if the alveolar rim showed localized sites of erosion. Additionally, we included simple qualitative observations regarding the position of the crista zygomaticoalveolaris (or its prolongation towards the alveolar process) relative to tooth position (see Tab. 1, last column).

We also included a landmark in the middle of the mandibular fossa to capture the spatial relationship between the maxilla and the temporomandibular joint (TMJ). Biomechanically this is interesting since compressive forces are dissipated via the fossae into the temporal bone at the end of the zygomatic arch. The fossa is a clearly defined area in some individuals, but can be difficult to delimit in others (particularly apes). It can thus not be identified with high precision. Moreover, the TMJ was not accessible in multiple cases on casts (Tab. 1, column TMJ). For this reason the TMJ data set was analyzed separately.

Ten semilandmarks were equally distributed along each alveolar rim curve, and a set of five semilandmarks was placed in the superior region of the ZAC. Sliding of the semilandmarks was performed in the EVAN Toolbox 1.71 (ET; http://evan-society.org) and based on the minimum bending energy approach (Bookstein 1989; Gunz et al. 2005; Gunz and Mitteroecker 2013). Cartesian coordinates were converted into shape variables by means of a Generalized Procrustes Analysis (GPA; Gower 1975; Marcus et al. 1996), which eliminates variation in orientation, location, and size. Shape variables were then analyzed via Principal Component Analysis (PCA) to reduce dimensions. Shape changes were visualized by Thin Plate Spline warping (TPS; Bookstein 1978, 1991) in the EVAN Toolbox 1.71. Size was analyzed separately using the natural log of Centroid Size (lnCS; Centroid Size is the square root of the sum of squared distances of a set of landmarks from their centroid). Allometry (shape changes related to size) was determined by multivariate linear regression using all shape variables as dependent variables and lnCS as independent variable in the EVAN Toolbox 1.71.

RESULTS

In shape space the first three Principal Components (PCs) explain 39.2%, 32.4%, and 6.4% of the total variance. Fig. 3 shows the plot for the first two PCs and includes the related shape changes in top view at each extreme of the distribution. Analogously, Fig. 4 provides a frontal view of the ZAC shape. Changes along PC1 account for a more anterior placement of the zygomatic root relative to the dental arch versus a more posterior placement. Shape changes of the ZAC are subtle and related with a flexed ZAC in the region of the malar tubercle (cf. Pope 1991) vs. a well-rounded shape. PC2 is associated with the relative height of the ZAC, i.e. the vertical distance between zygomaxillare and the dental arch (tall or short), with the shape of the ZAC (curved or steeply inclined), and with the transverse width of the posterior tooth row in relation to the anterior one (only slightly broader posteriorly or markedly broader posteriorly).

However, the individual hominid groups separate far less than anticipated. Chimpanzees, gorillas, and orangutans plot at the lower border of the modern human distribution, with a partial overlap. Australopithecines are separated from the great apes along PC2 for their higher and steeply inclined ZAC, and their broader posterior dental arch but the *Au* distribution partly overlaps with modern humans as well because of *Au. sediba*. Habilines, Erectines, Mid-Pleistocene hominins, early anatomically modern humans, and upper Paleolithic humans are within or in the close vicinity of the central shape distribution of modern humans. Most Australopithecines, and particularly Paranthropines and Neanderthals separate from this cluster. *Pa* and some *Au* (A.L. 444-2, Sts 71) for their relatively high and steeply inclined ZAC, broad postcanine tooth row, and for their forwardly positioned zygomatic root in some cases (OH5, SK12), *NEA* because of their backwardly positioned and

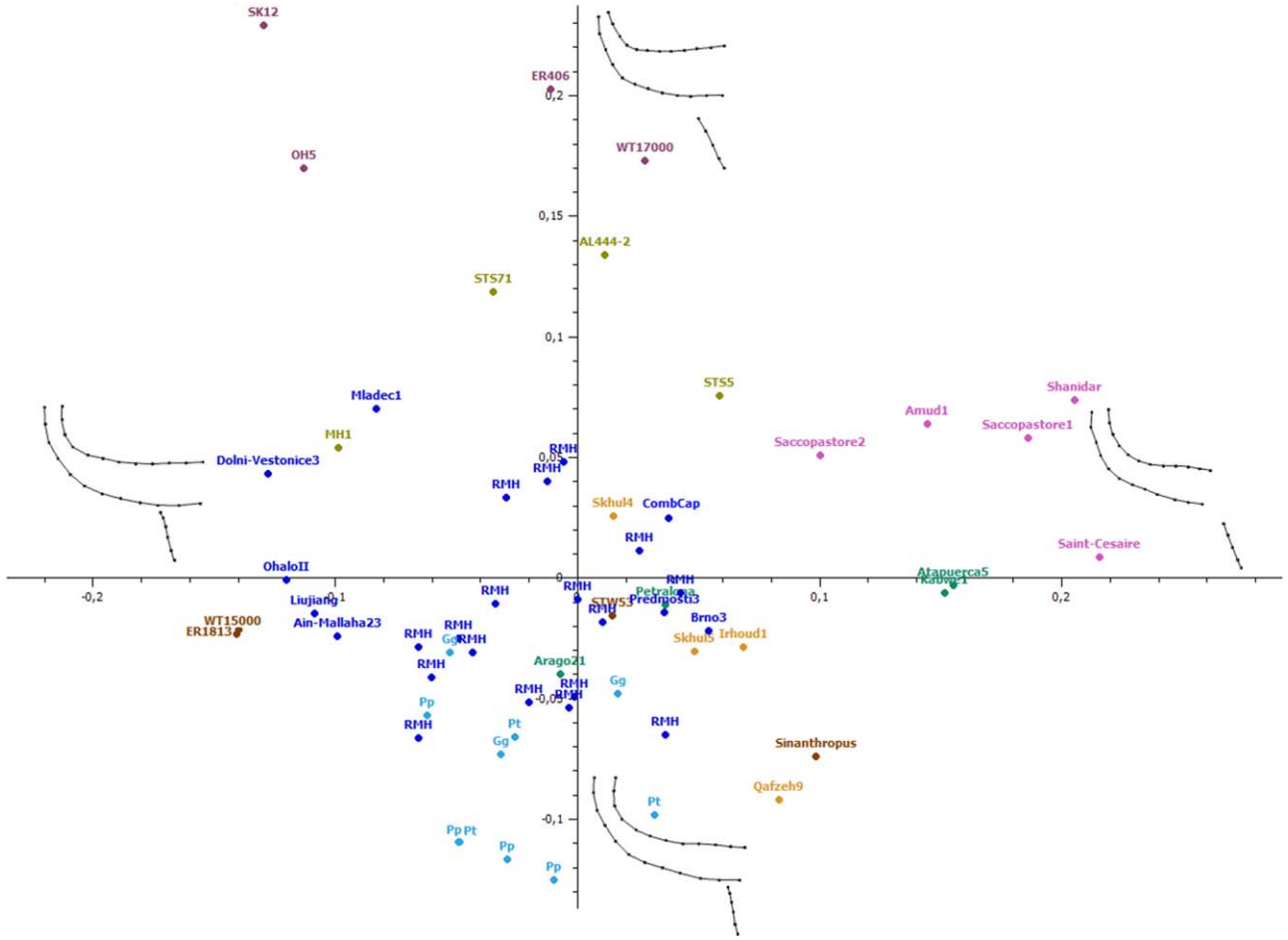

Fig. 3. The first two Principal Components of shape space for the landmark/semilandmark set shown in Fig. 2, and associated shape changes in top view at the extremes of the distribution. Coloring of specimens according to grouping in Tab. 1.

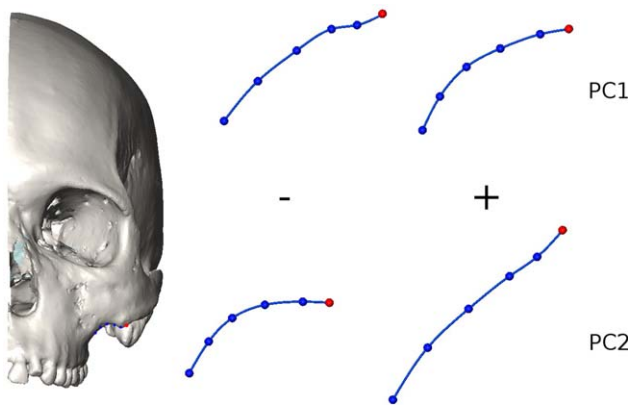

Fig. 4. Associated shape changes for the ZAC curve (C01) in frontal view at the extremes of the shape distribution.

swept back zygomatic root but featuring a moderate ZAC height. The *NEA* subsample is very clearly separated from modern humans along PC1, and so is the Sima des los Huesos (SH) specimen Atapuerca 5, and the Zambian fossil Kabwe 1. *eAMH* form an interesting elongated cluster between *NEA* and the majority of modern humans. Their zygomatic root is generally located rather far back relative to the dentition (PC1) but a high degree of variation is observed with regard to the features associated with PC2. The Levantine specimens Skhul 4, Skhul 5 and Qafzeh 9 are quite different along PC2, Jebel Irhoud 1 is similar to Skhul 5.

An obvious evolutionary pattern over time, i.e. from Australopithecines to Habilines, Erectines, *MPH*, and further on to *eAMH* and *RMH* is not suggested. Only apes and Australopithecines/Paranthropines seem to be separated consistently by their ZAC height (low in apes, high in *Au*/*Pa*), ZAC shape (curved in apes, steeply inclined in *Au*/*Pa*), and relative width of the posterior teeth in relation to the anterior (more equal in apes, broad in *Au*/*Pa*).

We performed other analyses removing the curve semilandmarks. Results are very similar (Fig. 5), just the apes and Sts 71 move a bit closer into the modern human distribution. This means that a lot of the signal is preserved in a limited configuration of only five landmarks.

Including the TMJ, however, changes the picture slightly (Fig. 6). PC1 and PC2 are exchanged. The apes

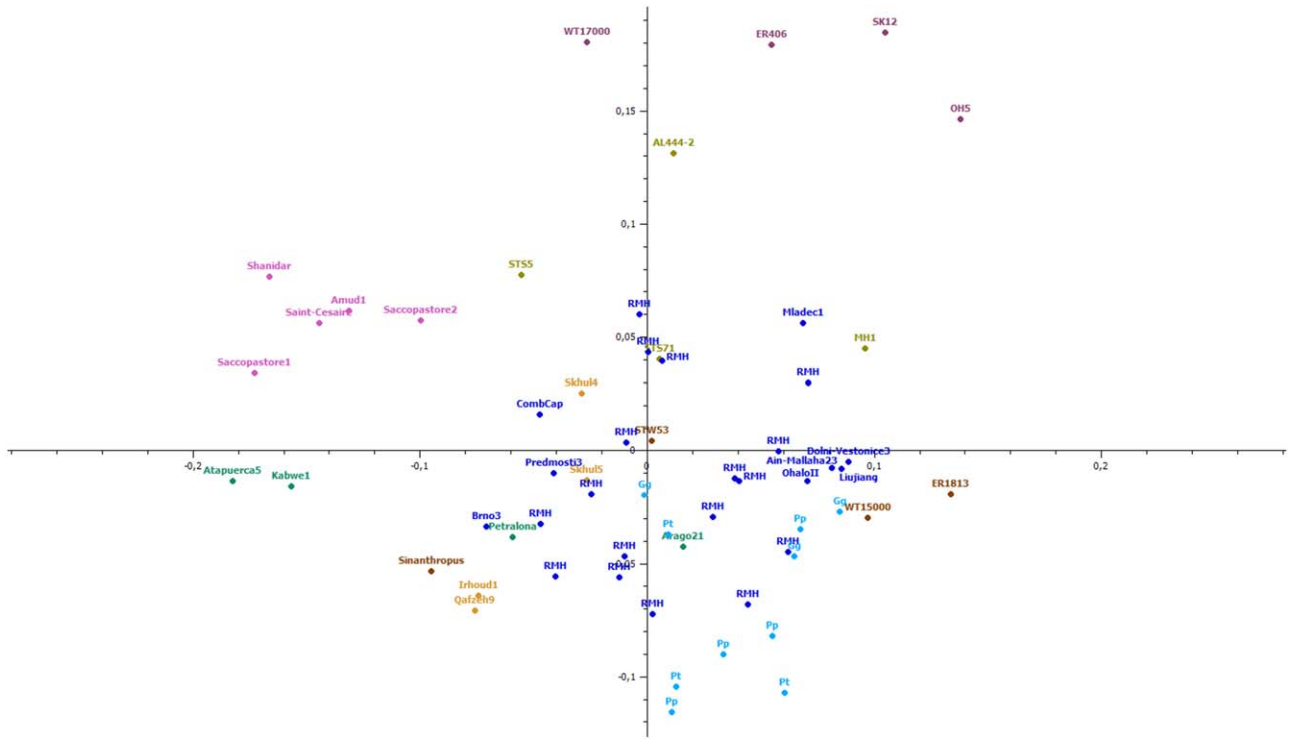

Fig. 5. The first two Principal Components of shape space for the set of five landmarks only [pr, ol, zm, lingual and buccal midpoint of second molar (M^2) alveoli]. Coloring of specimens according to grouping in Tab. 1.

are now separated along PC1 from *Homo*, owing to a shorter anterior/posterior but increased vertical distance between the zygomatic root and the TMJ. *Au* and *Pa* plot on the other end of the distribution, which is due to a relatively larger anterior/posterior but reduced vertical distance between zygomatic root and TMJ. Only MH1, assigned to *Au.sediba*, is plotting utterly within the *RMH*s. Amud 1 and Atapuerca 5 are still located far from the other hominins for their backward position of the zygomatic root and the smaller distance of the latter to the TMJ. Unfortunately the TMJ sample is reduced and lacking any other *NEA* (see Materials and Methods).

The lnCS of the complete landmark/semilandmark configuration was used as a three-dimensional measurement for size (Fig. 7). As expected, modern humans are smallest, and outside the size range of *NEA* and *MPH*. *eAMH* are larger than most RMH but smaller than NEA. *MPH* are in the same size range as *NEA, Er* and *Ha* are smaller than *Au*. Apes and *Pa* are the largest. When apes, gracile and robust Australopithecines are included in the sample, only 5.4% of shape variance can be explained by lnCS. However, if only the genus *Homo* (from Habilines to recent modern humans) is considered, this percentage increases to 32.1%. The fact that size is an important explanatory factor for shape in our genus is to a large extent based on the pronounced size differences between RMH on the one hand and NEA/MPH on the other. Large size is associated with a more backwardly positioned zygomatic root and a higher and steeply inclined ZAC, small size with the opposite, i.e. a more forwardly and low positioned zygomatic root and a curved ZAC. It is important to note that "size" here reflects only the size of the captured maxillary region, not of the entire cranium.

DISCUSSION

This contribution is an attempt to describe a particular aspect of the hominid maxilla using state-of-the-art Geometric Morphometric methods. We focused on the zygomatic root of the maxilla and its spatial relationship to the dental arch. Since this region is exposed to considerable stresses and strains during chewing, the different dietary strategies of various hominid groups might have led to characteristic shapes that could be helpful for classification. The outcome of our pilot study is threefold:

1. No clear pattern of shape can be found to allow separating the highly variable modern humans from other extant and extinct hominid groups with confidence, except from two extreme forms – Paranthropines and Neanderthals.
2. There is no clear trend over time. The quite distinct maxillary morphologies of Paranthropines and Neanderthals appear at different times and stages of human evolution. Other hominins from roughly the last two million years such as Habilines, Erectines, and Middle Pleistocene *Homo* can be very similar to modern humans. Even apes and Australopithecines are within or not far from the central shape distribution of *Homo*. Nevertheless, great apes, gracile

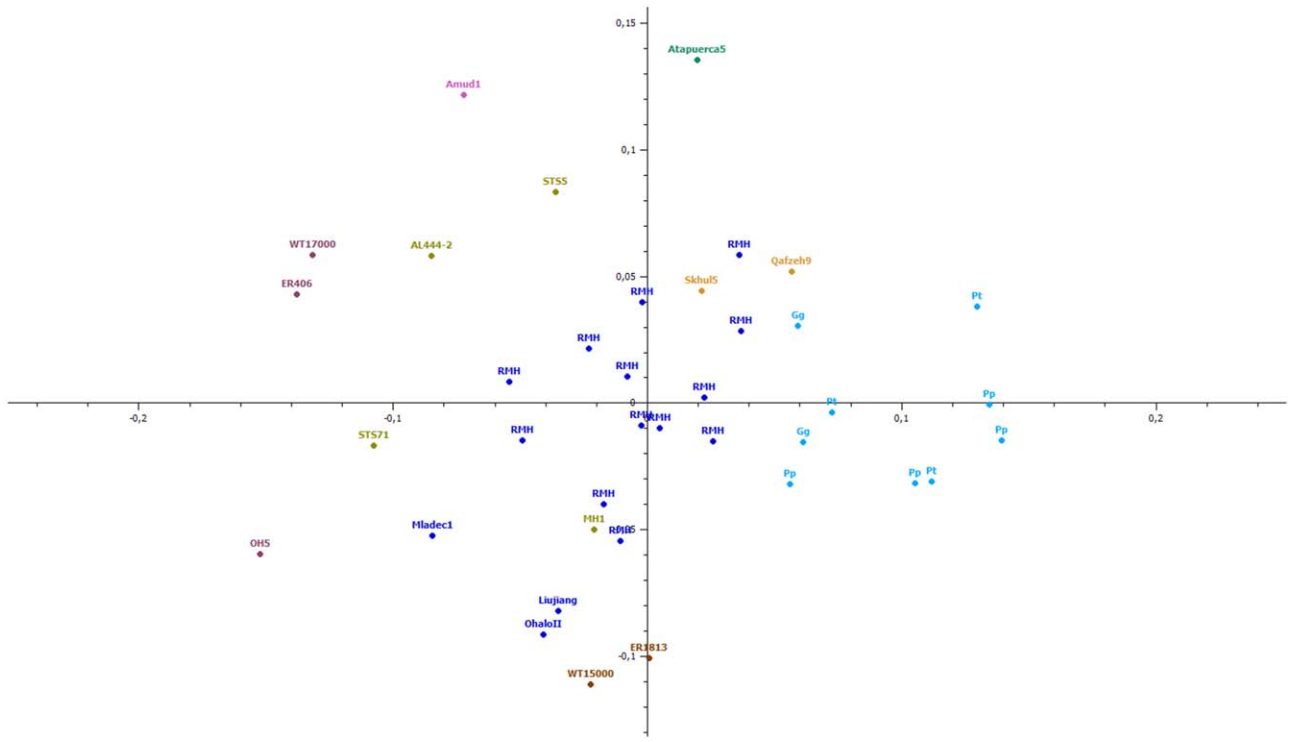

Fig. 6. The first two Principal Components of shape space for the landmark/semilandmark set shown in Fig. 2 plus a landmark in the middle of the mandibular fossa (TMJ). Coloring of specimens according to grouping in Tab. 1.

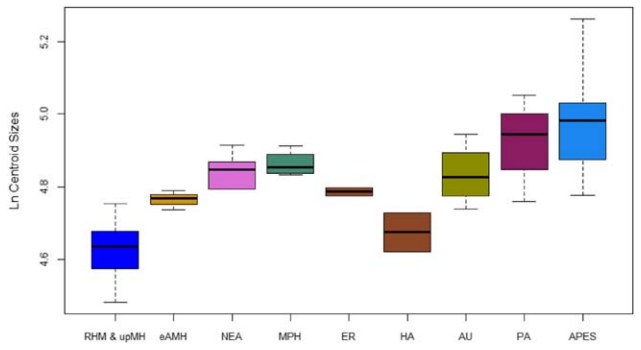

Fig. 7. Boxplot of the natural logarithm of Centroid Size (lnCS) for the included hominid groups.

Australopithecines, and Paranthropines are separated from each other by shape factors related to PC2 (see results).

3. The geometry studied here allows simple measurements and analyses and is thus potentially interesting for the scientific community to distinguish at least the two extreme forms from the rest of the hominids. This is, for instance, useful for fragmentary Late Pleistocene remains with an unclear affiliation to either *NEA* or *AMH*.

Recently, Lacruz and colleagues (2015) have summarized growth patterns of the Neanderthal maxilla. The deposition and resorption of bone (bone growth remodeling) is an essential mechanism in this developmental process. By mapping remodeling fields, they found extensive bone deposition in Neanderthals and Sima des los Huesos hominins, but mainly resorptive activities in modern human anterior maxillae. The latter state is associated with a retracted face positioned largely under the braincase. *Au. afarensis*, *Au. africanus* and early *Homo* show similarly extensive bone deposition over the maxillae (Bromage 1989; Bromage and Boyde 2008; McCollum 2008; Lacruz et al. 2013). These observations would explain the differences between *NEA* and modern humans, but not between *NEA* and the other hominins. Still, our results show that *NEA* clearly feature a distinct morphology in comparison to all other hominid groups, namely a zygomatic root that is located far back, swept back, and moderately high above the dental arch. The SH cranium 5 is quite similar to *NEA* and distinct from the others. This is in agreement with claims that the SH group represents an early form of *NEA* that shows a lot of derived traits, sometimes more than classic Neanderthal (Martinón-Torres et al. 2016). Kabwe 1 is interestingly similar to SH cranium 5 for the features studied here, although it shows other distinct traits that are not present in the SH sample (e.g., Seidler et al. 1997). In contrast to the view that the Neanderthal face is not derived but rather a plesiomorphic extension of a former trend (Trinkaus 2003), the very distinct morphology we found in our study for *NEA* calls for a re-evaluation of this hypothesis. *eAMH* are different from *NEA* for their slightly more forwardly placed zygomatic

root but show a larger variation with regard to ZAC height and shape, and relative width of the posterior dental arch. Our results corroborate other findings (Freidline et al. 2012) suggesting a more modern facial morphology of Jebel Irhoud 1.

The three ape genera are not systematically different in our results. There is a trend for a weak separation of *Pongo* from the African apes, but it is not consistent. A larger sample in future works should clarify this further. For the purpose of this paper, however, it is sufficient to detect the principal shape similarities/differences to other hominids. In this sense, apes are not so much different from *Au* and *Pa* for their anterior/posterior position of the zygomatic root relative to the dental arch (except some special forms such as OH5, SK12, and probably MH1, see PC1 Fig. 3), but they differ substantially for their lower maxillary height, more curved ZAC shape, and the narrower postcanine tooth row. Starting from their last common (and unknown) ancestor, apes and *Au* took divergent pathways of shape development, and *Pa* might be an extension or exaggeration of the *Au* shape trajectory. Looking at the face from a frontal view, a greater portion of the *Pa* face is below the zygomatic arches rather than above it, which results in a high placing of the zygomatic arches relative to the occlusal plane (Lieberman 2011). Our data fully confirms this configuration and indicates that A.L. 444-2 and Sts 71 are those representatives of *Au* in our sample which come closest to the *Pa* status (cf. e.g. Clarke 2008). Note that the term "prognathism" in its usual sense (the protrusion of the lower face relative to the upper face) is only applicable with restrictions to our dataset since we focus just on the dental arch and the zygomatic root. *Au. africanus* is less prognathic than earlier *Au*, WT-17000 has an extremely large and prognathic face. However, the relative anterior/posterior position of the zygomatic root to the dentition is not very different.

Early *Homo* has experienced a marked reduction in postcanine tooth area between *Ha* and *Er*, while *Ha* have only slightly smaller postcanine teeth than *Au* (McHenry & Coffing 2000). We find quite different shapes for the few *Ha* and *Er* specimens in our sample, but they are all within the shape distribution of later *Homo* and not systematically different from them. The picture would not change if we would re-label some of the fossils, as for instance would be possible for Stw 53 (see Kuman and Clarke 2000 vs. Curnoe and Tobias 2006). ER-1813 and WT-15000, both assigned to different species, are strikingly similar in our data set.

The TMJ on the working and the balancing (non-biting) side together with the bite point (e.g., M^2) form a triangle of support. The resultant vector of the jaw adductor muscles should pass through this triangle to produce compressive forces at all three points (Ledogar et al. 2016a). If this is not the case, distractive forces at the working side TMJ would occur, for which this joint is generally not well adapted. To avoid this situation, mammals reduce the activities of muscles on the balancing side, which means at the same time to decrease bite force. Beside the recruitment of muscles, the spatial configuration of the TMJ relative to the dentition is of course crucial. Where possible, we included a landmark at the TMJ in our sample. The results of this smaller sample (see Material and Methods) are not systematically different from those without TMJ but the distribution of apes is then separated from that of *Homo*, just like those of *Pa*, most *Au* (except MH 1), and *NEA*.

The zygomatic root of apes is located relatively closer to the TMJ in anterior/posterior direction, but their zygomatic root is low above the occlusal plane and thus the vertical distance to the TMJ is increased. *Pa*, and to some extent *Au*, feature exactly the opposite configuration, i.e. their zygomatic root is farer away from the TMJ anterior-posteriorly but since the root is higher above the occlusal plane, the vertical distance to the TMJ is decreased. *NEA* and the few *Ha*/*Er* left in this analysis are likewise on opposite shape trends that include the distance of the zygomatic root to the TMJ. The analysis suggests the presence of a few crucial shape factors:

- vertical distance between the zygomatic root and dental arch
- vertical distance between the zygomatic root and TMJ, and
- anterior/posterior distance between the zygomatic root and TMJ.

It is reasonable to assume that these features are highly interrelated and would limit each other. For instance, the superficial head of the masseter *must* run down diagonally to the angle of the mandible to allow also for protrusion (beside elevation), and the resultant vector of adductor muscles *must* be kept within the triangle of support if bite force is to be produced efficiently. Such different configurations could be tested in biomechanical simulations using finite element models, as for instance shown in the contribution of Ledogar and colleagues in this volume (2016b) for a limited set of configurations (Sts 5, MH 1, and variants produced from them). The simulations showed that a more anteriorly-positioned zygomatic root led to greater efficiency in producing bite forces because of a higher mechanical advantage compared to a posterior root. However, if only the zygomatic root is moved forward this might result in TMJ distraction. A straight and steeply inclined ZAC reduces strain magnitudes across facial regions, thus structurally reinforcing the face, while a more anteriorly positioned zygomatic root leads, against predictions, to larger strain magnitudes, even if a straight and steep ZAC is present. So there are indications that the ZAC might act as a buttressing feature (Rak 1983) but many open questions still remain, e.g., if this can be shown for other forms of hominids from apes to modern humans, why the ZAC in many cases is a sharp ridge rather than a blunt swelling although no muscles insert there, and which role size plays?

Facial shape is certainly connected to feeding behavior. An attempt to relate diet with cranial shape was recently made by Noback and Harvati (2015) using modern humans with different subsistence strategies. They found no connection between diet and shape of the zygomatic root, as well as no correlation between diet and dental arch shape. However, their data indicated that the relative positioning of the dentition is more important than its shape. Although shape variation among modern humans is undoubtedly smaller than in our sample of hominids, these results are interesting and support our list of crucial shape factors above. To what extent genes influence the development of the zygomatic

arch is little known but in her study on the correlation between cranial bones, genes, and climate Von Cramon-Taubadel (2009) found that all cranial regions significantly correlate with climate, except the zygomatic bone. Only a low correlation with genetic data was detected for zygomatic bone, maxilla, and occipital.

Our sample in this study is small and preliminary. It nevertheless shows a stunning overlap in shape variation for the zygomatic root in relation to the dentition in many of the studied hominid groups. They are different for their overall cranial morphologies, and many of them also with regard to their feeding strategies. Nevertheless, only a few of these groups deviate from a predominant pattern of variation in the center of the shape distribution. This would be in agreement with the idea of a general "Bauplan" for the architecture of a quite crucial maxillary region that can basically be captured by only five landmarks. The evolutionary dead end *Paranthropines*, and the likewise extinct Neanderthals are the only markedly deviating groups. Their particular shape can be used for classification attempts. We hope that the findings in our study will stimulate further research with regard to genetic control of maxillary/zygomatic growth, and biomechanical simulation experiments.

ACKNOWLEDGMENTS

We thank Israel Hershkovitz and Julia Abramov (Tel Aviv University), George Koufos (Aristotle University of Thessaloniki), Juan-Luis Arsuaga (Universidad Complutense de Madrid), Lee Berger (University of the Witwatersrand), Fred Spoor (University College London, MPI Leipzig) and Emma Mbua (National Museums of Kenya), Phillip V. Tobias, Francis Thackeray (University of the Witwatersrand) and Stephanie Potze (Transvaal Museum), Cassian Magori (Bugando University College of Health Sciences Mwanza), Donatius Kamamba (Dept. of Antiquities Dar-es-Salaam) and Charles Sanane (University of Dar-es-Salaam), Ato Jara (ARCCH Addis Ababa) and Horst Seidler (University of Vienna), Chris Stringer and Rob Kruszynski (Natural History Museum London), Xinzhi Wu and Yaming Cui (IVPP Beijing) for access to fossils, respectively for scanning fossils. Gerlinde Gruber (Medical University Vienna), Maria Teschler-Nicola, Frank Zachos, and Eduard Winter (Natural History Museum Vienna) granted access to fossil and recent hominids, and fossil casts, and Katarina Matiasek provided background information on the collections from the Dept. of Anthropology, University of Vienna. We thank Martin Dockner for support during μCT scanning, Roman Ginner for taking photographs. We are grateful to Fred Bookstein and Cinzia Fornai for discussion and comments. This research was supported by the Department of Anthropology at University of Vienna, and the Oesterreichische Nationalbank, Anniversary Fund, project number 16121.

LITERATURE CITED

Benazzi S, Bookstein FL, Strait DS, Weber GW. 2011. A new OH5 reconstruction with an assessment of its uncertainty. J Hum Evol 61:75–88.

Bookstein FL. 1978. The Measurement of Biological Shape and Shape Change. Lecture Notes in Biomathematics Vol. 24. New York: Springer-Verlag.

Bookstein FL. 1989. Principal warps: Thin plate splines and the decomposition of deformations. IEEE Trans Pattern Anal Machine Intelligence 11:567–585.

Bookstein FL. 1991. Morphometric tools for landmark data: geometry and biology. [Orange Book]. Cambridge, New York: Cambridge University Press.

Brace CL, Rosenberg KR, Hunt KD. 1987. Gradual change in human tooth size in the Late Pleistocene and post-Pleistocene. Evolution 41:705–720.

Bromage TG. 1989. Ontogeny of the early hominid face. Journal of Human Evolution 18:751–773.

Bromage T, Boyde A. 2008. Bone growth remodeling of the early human face. In: Enlow DH, Hans MG, editors. Essentials of facial growth. Ann Arbor, MI: Needham Press. p 319–342.

Clarke RJ. 2008. Latest information on Sterkfontein's Australopithecus skeleton and a new look at Australopithecus. South African Journal of Science 104:443–449.

Curnoe D, Tobias PV. 2006. Description, new reconstruction, comparative anatomy, and classification of the Sterkfontein Stw 53 cranium, with discussions about the taxonomy of other southern African early Homo remains. Journal of Human Evolution 50:36–77.

Demes B, Creel N. 1988. Bite force, diet, and cranial morphology of fossil hominids. Journal of Human Evolution 17:657–670.

Fleagle JG, Gilbert CC, Baden AL. 2010. Primate cranial diversity. American Journal of Physical Anthropology 142:565–578.

Freidline SE, Gunz P, Harvati K, Hublin JJ. 2012. Middle Pleistocene human facial morphology in an evolutionary and developmental context. Journal of Human Evolution 63:723–740.

Gower JC. 1975. Generalized procrustes analysis. Psychometrika 40:33–51.

Gunz P, Mitteroecker P, Bookstein FL. 2005. Semilandmarks in three dimensions. In: Slice DE, editor. Modern Morphometrics in Physical Anthropology. New York: Kluwer Press. p 73–98.

Gunz P, Mitteroecker P. 2013. Semilandmarks: A method for quantifying curves and surfaces. Hystrix 24:

Hylander WL. 1977. The adaptive significance of Eskimo craniofacial morphology. In: Dahlberg AA, Graber TM, editors. Orofacial Growth and Development. The Hague, Paris: Mouton Publishers. p 129–169.

Kuman K, Clarke RJ. 2000. Stratigraphy, artefact industries and hominid associations for Sterkfontein, Member 5. Journal of Human Evolution 38:827–847.

Lacruz RS, de Castro JMB, Martinón-Torres M, O'Higgins P, Paine ML, Carbonell E, Arsuaga JL, Bromage TG. 2013. Facial Morphogenesis of the Earliest Europeans. PLoS ONE 8:

Lacruz RS, Bromage TG, O'Higgins P, Arsuaga JL, Stringer C, Godinho RM, Warshaw J, Martínez I, Gracia-Tellez A, De Castro JMB, etal. 2015. Ontogeny of the maxilla in Neanderthals and their ancestors. Nature Communications 6:

Ledogar JA, Smith AL, Benazzi S, Weber GW, Spencer MA, Carlson KB, McNulty KP, Dechow PC, Grosse IR, Ross CF, etal. 2016a. Mechanical evidence that Australopithecus sediba was limited in its ability to eat hard foods. Nature Communications 7:1–9.

Ledogar JA, Benazzi S, Smith AL, Weber GW, Grosse I, Ross C, Richmond BG, Wright BW, Byron C, Strait DS, Wang Q, Dechow P. 2016b (in review). The biomechanics of bony facial "buttresses" in South African australopiths: an experimental study using finite element analysis. Anat Record. (in review). DOI 10.1002/ar.23492

Lieberman DE, Krovitz GE, Yates FW, Devlin M, St. Claire M. 2004. Effects of food processing on masticatory strain and craniofacial growth in a retrognathic face. Journal of Human Evolution 46:655–677.

Lieberman DE. 2008. Speculations about the selective basis for modern human craniofacial form. Evolutionary Anthropology 17:55–68.

Lieberman DE. 2011. The Evolution of the Human Head. Cambridge MA: The Belknap Press of Harvard University Press.

Lucas PW. 2004. Dental Functional Morphology - How Teeth Work. Cambridge: Cambridge University Press.

Marcus LF, Corti M, Loy A, Naylor G, Slice DE. 1996. Advances in morphometrics. [White Book]. New York: Plenum Press.

Martinón-Torres M, Xing S, Liu W, Bermúdez de Castro JM. 2016. A "source and sink" model for East Asia? Preliminary approach through the dental evidence. Comptes Rendus - Palevol. DOI: 10.1016/j.crpv.2015.09.011.

McCollum MA. 2008. Nasomaxillary remodeling and facial form in robust Australopithecus: a reassessment. Journal of Human Evolution 54:2–14.

McHenry HM, Coffing K. 2000. Australopithecus to Homo: Transformations in body and mind. In: Annual Review of Anthropology 125–146. p

Noback ML, Harvati K. 2015. The contribution of subsistence to global human cranial variation. Journal of Human Evolution 80:34–50.

Pope GG. 1991. Evolution of the zygomaticomaxillary region in the genus Homo and its relevance to the origin of modern humans. Journal of Human Evolution 21:189–213.

Rak Y. 1983. The Australopithecine Face. New York, London: Academic Press.

Rak Y. 1986. The Neanderthal: A new look at an old face. Journal of Human Evolution 15:151–164.

Seidler H, Falk D, Stringer C, Wilfing H, Muller GB, zur Nedden D, Weber GW, Reicheis W, Arsuaga JL. 1997. A comparative study of stereolithographically modelled skulls of Petralona and Broken Hill: implications for future studies of middle Pleistocene hominid evolution. J Hum Evol 33:691–703.

Trinkaus E. 1987. The Neandertal face: evolutionary and functional perspectives on a recent hominid face. Journal of Human Evolution 16:429–443.

Trinkaus E. 2003. Neandertal faces were not long; modern human faces are short. Proceedings of the National Academy of Sciences of the United States of America 100:8142–8145.

Ungar PS, Grine FE, Teaford MF. 2006. Diet in early Homo: A review of the evidence and a new model of adaptive versatility. In: Annual Review of Anthropology 209–228. p

Ungar PS. 2012. Dental evidence for the reconstruction of diet in African early Homo. Current Anthropology 53:S318–S329.

Von Cramon-Taubadel N. 2009. Congruence of individual cranial bone morphology and neutral molecular affinity patterns in modern humans. American Journal of Physical Anthropology 140: 205–215.

Weber GW, Bookstein FL. 2011. Virtual Anthropology - A Guide to a New Interdisciplinary Field. Wien, New York: Springer Verlag. ISBN 978-3-211-48647-4.

Weber GW. 2015. Virtual Anthropology. Yearbook of Physical Anthropology 156:22–42.

Witzel U, Preuschoft H, Sick H. 2004. The role of the zygomatic arch in the statics of the skull and its adaptive shape. Folia Primatologica 75:202–218.

Wrangham RW, Jones JH, Laden G, Pilbeam D, Conklin-Brittain N. 1999. Cooking and the ecology of human origins. Current Anthropology 40:567–594.

Wrangham R, Carmody R. 2010. Human adaptation to the control of fire. Evolutionary Anthropology 19:187–199.

Zink KD, Lieberman DE, Lucas PW. 2014. Food material properties and early hominin processing techniques. Journal of Human Evolution 77:155–166.